[10] Representative recent calculations on Cope rearrangements: a) D. J. Tantillo, R. Hoffmann, *J. Org. Chem.* **2002**, in press; b) O. Wiest, K. A. Black, K. N. Houk, *J. Am. Chem. Soc.* **1994**, *116*, 10336 – 10337; c) H. Jiao, P. von R. Schleyer, *Angew. Chem.* **1995**, *107*, 329; *Angew. Chem. Int. Ed. Engl.* **1995**, *34*, 334 – 337.
[11] A. P. Scott, L. Radom, *J. Phys. Chem.* **1996**, *100*, 16502 – 16513.
[12] Only "chairlike" (as opposed to "twist") isomers[13] of 1,5-cyclooctadiene substructures were considered due to the geometric constraints of the polymers.
[13] Experiments and force-field calculations on 1,5-cyclooctadiene: a) G. M. Whitesides, G. L. Goe, A. C. Cope, *J. Am. Chem. Soc.* **1967**, *89*, 7136 – 7137; b) D. Boeckh, R. Huisgen, H. Noeth, *J. Am. Chem. Soc.* **1987**, *109*, 1248 – 1249; c) N. L. Allinger, J. T. Sprague, *J. Am. Chem. Soc.* **1972**, *94*, 5734 – 5747.
[14] Barriers for Cope rearrangement of species with terminal acyclic hexadiene units were found to converge rapidly upon cyclobutane fusion to approximately 30 kcal mol^{-1} (from 42 kcal mol^{-1} in the parent boatlike cyclohexadiene,[10] Scheme 2). Also, [*n*]-ladderane oligomers were generally found to be < 4 kcal mol^{-1} more stable than the broken [*n*]-ladderane isomers with central cyclooctadiene substructures derived from them (i.e. those species whose relative energies are set to 0.0 in Scheme 2).
[15] We have not yet investigated substituent effects on this rearrangement; appropriately designed, they may lower the barrier even further.
[16] a) R. Pettit, J. S. McKennis, L. Brener, J. S. Ward, *J. Am. Chem. Soc.* **1971**, *93*, 4857 – 4958; b) previous calculations predict similar rearrangement barriers: B. Das, K. L. Sebastian, *Chem. Phys. Lett.* **2000**, *330*, 433 – 439, and references therein.
[17] a) N. C. C. Yang, B. J. Hrnjez, M. G. Horner, *J. Am. Chem. Soc.* **1987**, *109*, 3158 – 3159; b) N. C. C. Yang, M. G. Horner, *Tetrahedron Lett.* **1986**, *27*, 543 – 546; c) HF/6-31G* calculations on the structure and energy of **7** relative to other $C_{12}H_{12}$ isomers have also been reported: G. W. Schriver, D. J. Gerson, *J. Am. Chem. Soc.* **1990**, *112*, 4723 – 4728.
[18] Such systems include, for example, the asteranes[1a]—isomers of large prismanes with combinations of *cis* and *trans* fused cyclobutanes.
[19] The size of these molecules has, so far, precluded computations on their putative fluxionality.

Ultrastable and Highly Acidic, Zeolite-Coated Mesoporous Aluminosilicates**

Do Trong On and Serge Kaliaguine*

The acidity and hydrothermal stability of mesoporous aluminosilicates (MesoAS) are relatively low compared to those of zeolites, which limits their potential applications as catalysts in petroleum refining and fine chemicals synthesis.[1–7] Much effort has therefore been undertaken to synthesize a new type of materials, which combines the advantages of both zeolites and mesoporous molecular sieves. One might expect to improve both the stability and acidity of these materials if zeolite-like order could be introduced into the mesopore walls. Recent advances showed that amorphous walls of the mesostructure could indeed be converted to a partially zeolitic product.[8–13] For example, MCM-41/MFI composites containing interconnected mesopores and micropores were prepared by using dual templates and exhibited enhanced acidity and steam stability compared to the corresponding MCM-41.[8, 9] Furthermore, the use of zeolite seeds as precursors for the assembly of mesoporous aluminosilicates with high hydrothermal stability and acidity was reported by Pinnavaia et al.[10] A similar zeolite beta type of materials was also prepared in the presence of co-templates of tetraethylammonium hydroxide and cetyltrimethylammonium bromide.[11] Recent results from our group showed the preparation of a new type of materials with semicrystalline zeolitic mesopore walls based on a templated solid-state secondary crystallization of zeolites starting from the amorphous walls of SBA-15. Bright- and dark-field transmission electron microscope (TEM) images recorded on the same area of the sample indicated that nanocrystals were embedded in the continuous amorphous inorganic matrix to form semicrystalline wall structures while preserving the mesoporous structure. The resulting mesoporous materials had much stronger acidity than those of the corresponding amorphous alumosilicates and a much improved hydrothermal stability.[12]

Herein, we describe a new approach for the production of unusual zeolite-coated mesoporous aluminosilicates (ZCMeso-AS) using diluted clear solutions containing primary zeolite units. Hydrothermally ultrastable and highly acidic ZCMeso-AS result owing to the nanocrystalline zeolitic nature of their pore wall surface. These features open new possibilities for using this type of materials as acid catalysts.

It is of special concern that due to the size of primary ZSM-5 units templated by tetrapropylammonium ions (2.8 nm in diameter),[13–14] the pore diameter of the mesoporous precursor molecular sieves should be higher than 30 Å. The methods in references [2] and [3] are therefore useful in this context for the preparation of mesoporous precursors, such as SBA-15 and siliceous mesostructured cellular foams (MCFs).

The N_2 adsorption/desorption isotherms obtained from the calcined sample before and after coating are shown in Figure 1 A. The parent and ZSM-5-coated samples display the typical behavior of a mesoporous molecular sieve with a mesopore volume saturation capacity of about 1.56 and 0.78 cm^3 g^{-1}, respectively (Table 1). The P/P_0 position of the inflection point is related to a diameter in the mesopore range, and the sharpness of these steps indicates the uniformity of the pore size. A narrower distribution of the pore diameter of the coated sample compared to that of the parent sample was observed (Figure 1 B). Furthermore, a significant decrease in pore diameter (from 70 to 54 Å) and in surface area (from 800 to 465 m^2 g^{-1}) could conceivably be ascribed to the ZSM-5 nanocrystals coated inside the mesopore channels of the host. Figure 2 shows a TEM image of the ZSM-5-coated MesoAS. A uniform pore size with a highly ordered structure is still observed for this sample after the coating procedure.

The ZSM-5-coated MesoAS sample shows a FTIR absorption band at 550 cm^{-1}, which is not present in the parent MesoAS sample (Figure 3). The band around 550 cm^{-1} has been assigned to the asymmetric stretching mode in double-

[*] Prof. S. Kaliaguine, Dr. D. Trong On
Department of Chemical Engineering
Laval University
Quebec G1K 7P4 (Canada)
Fax: (+1) 418-656-3810
E-mail: kaliagui@gch.ulaval.ca

[**] This work was supported by the Natural Sciences and Engineering Research Council of Canada (NSERC) through a strategic grant. We thank Dr. M. H. Zahedi-Niaki for the recording of NMR data.

  0044-8249/02/11406-1078 $ 17.50+.50/0

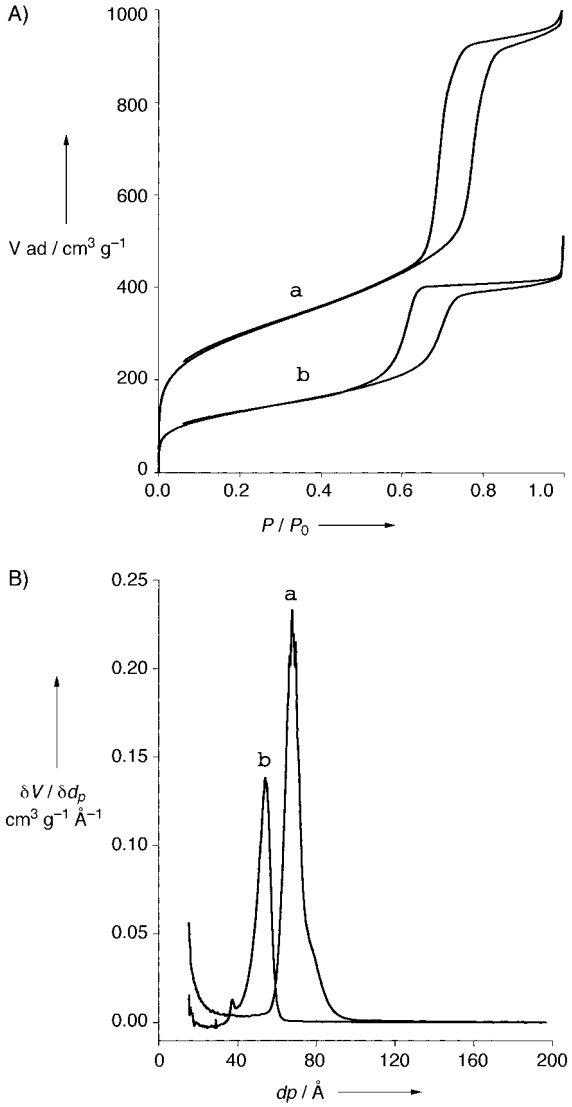

Figure 1. N_2 adsorption/desorption isotherms of nitrogen at $-196\,^{\circ}C$ (A) and Barrett–Joyner–Halenda (BJH) pore diameter distributions calculated from the desorption branch of the isotherm (B) for a) parent MesoAS, b) ZSM-5-coated MesoAS.

Tabelle 1. Physicochemical properties of the parent mesoporous aluminosilicate (PMesoAS) and ZSM-5-coated mesoporous aluminosilicate (ZCMesoAS) samples.

Entry	Materials	Si/Al[a]	S_{BET} [$m^2 g^{-1}$]	S_{BJH} [$m^2 g^{-1}$]	Mesopore volume [$cm^3 g^{-1}$]	BJH pore diameter [Å]
1	PMesoAS	65	1080	800	1.56	70
2	ZCMesoAS	50	495	465	0.78	54

[a] Atomic Si/Al ratios obtained by atomic adsorption spectroscopy.

Figure 2. TEM image of ZSM-5-coated MesoAS.

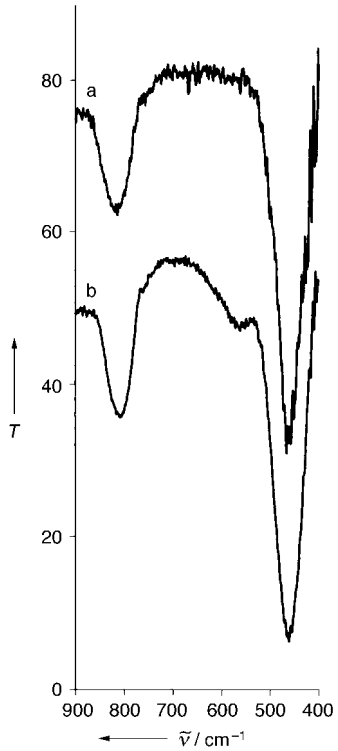

Figure 3. FTIR spectra of: a) parent MesoAS, b) ZSM-5-coated MesoAS.

ringblocks and is observed in all of the zeolite structures that contain the double 4-, double 5-, and double 6-rings (zeolite X, Y, A). Such a band was also assigned to the vibration associated with the five-membered ring in the pentasil secondary building units.[10] Its occurrence indicates therefore that ZSM-5 nanocrystals are present within the mesostructured material.

The FTIR spectra of adsorbed pyridine after desorption at $150\,^{\circ}C$ on the parent MesoAS (atomic Si/Al = 65/1) in H-form and H-ZSM-5-coated MesoAS (Si/Al = 50/1) samples and on H-ZSM-5 (Si/Al = 57/1) as the reference are shown in Figure 4 (the samples in H-form were obtained by the ion exchange of Na^+ by NH_4^+ followed by calcination at $550\,^{\circ}C$). Two intense bands at 1547 and 1455 cm^{-1}, which are characteristic of Brönsted and Lewis acid sites, respectively, are observed for the H-ZSM-5-coated MesoAS sample and the H-ZSM-5 reference; however, no such bands are observed for the parent MesoAS sample in H-form. This suggests that the

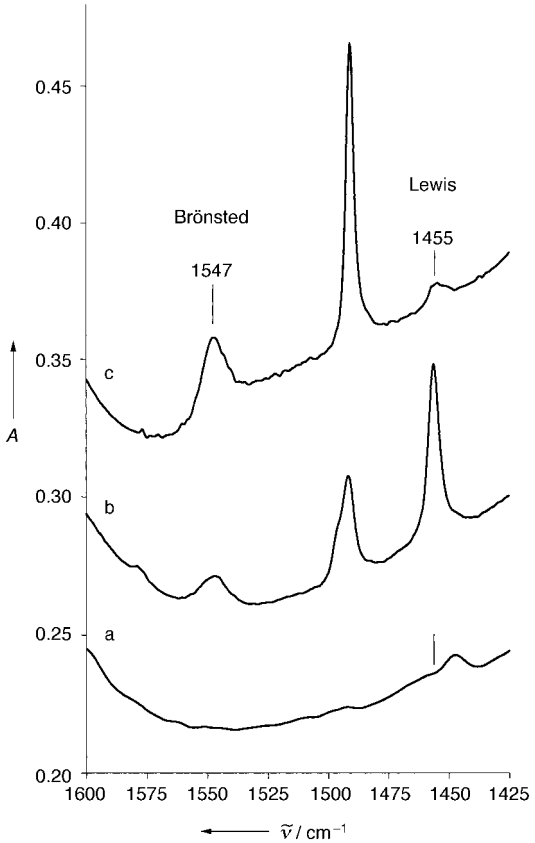

Figure 4. FTIR spectra of the adsorbed pyridine in the 1350–1600 cm^{-1} range after pyridine adsorption and then desorption at 150°C: a) parent MesoAS in H-form, b) H-ZSM-5-coated MesoAS, c) H-ZSM-5.

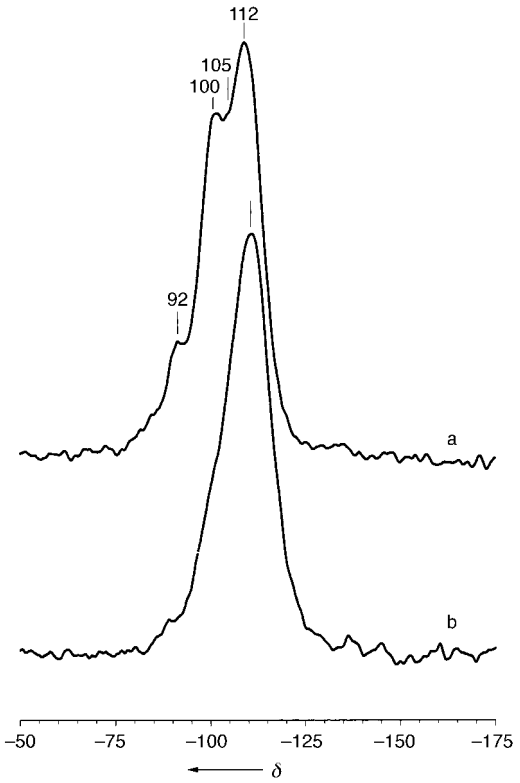

Figure 5. ^{29}Si MAS NMR spectra of: a) parent MesoAS, b) ZSM-5-coated MesoAS.

acidity of the coated sample is comparable to that of the H-ZSM-5 reference with a larger fraction of Lewis acid sites and much higher than that of the parent sample. The order of the acid site density is H-ZSM-5 > H-ZSM-5-coated MesoAS ≫ parent MesoAS.

The ^{27}Al MAS NMR spectra of the parent MesoAS and ZSM-5-coated samples exhibit a single resonance centered at about $\delta = 56$, which is characteristic of tetrahedral aluminum centers. This indicates that most of the aluminum is incorporated into the material framework. The ^{29}Si MAS NMR spectrum of the parent MesoAS sample (atomic Si/Al = 65/1) is typical of mesoporous alumosilicates (Figure 5); it contains four main features[7, 15] (Figure 5a). Two main resonances at $\delta = -112$ and -100 and a weak peak at $\delta = -92$ correspond to Si(OSi)$_4$ (Q^4), (HO)Si(OSi)$_3$ (Q^3), (HO)$_2$Si(OSi)$_2$ (Q^2) silicate species, respectively; a shoulder at $\delta = -105$ has been assigned to (AlO)$_1$Si(OSi)$_3$ species due to the tetrahedral aluminum structure. By contrast, the ^{29}Si MAS NMR spectrum of the coated sample (atomic Si/Al = 50/1) shows a main resonance centered at $\delta = -112$, which is attributed to Q^4 silicon of the silicalite framework and a shoulder (AlO)$_1$-Si(OSi)$_3$ band at $\delta \sim 105$ (Figure 5b). Only a weak resonance attributable to Q^3 silicon from surface hydroxy groups is observed at $\delta \sim 100$. The increase in intensity of the Q^4 resonance and concomitant decrease in intensity of the Q^3 and Q^2 resonances reflect the transformation of the hydrophilic surface of the precursor into a more hydrophobic one upon applying the coating procedure.

The hydrothermal stability in boiling water at 100°C and steam stability with 20% water vapor in N_2 at 800°C of the parent mesoporous molecular sieves (MMS) sample and the ZSM-5-coated MesoAS sample were also studied (Table 2). The pore diameter distributions of the parent MMS sample before and after treatment in boiling water at 100°C for 48 h are shown in the inset in Figure 6A. The mesopore structure of the parent MesoAS sample had collapsed after this treatment for 48 h. By contrast, no significant collapse of the mesopore structure was observed for the ZSM-5-coated MMS sample after 48 h under the same treatment conditions. The pore volume and BJH surface area varied slightly from 0.78 to 0.85 cm^{3}g^{-1} and from 465 to 485 m^{2}g^{-1}, respectively (Figure 6A); even after 120 h, the mesopore structure was

Tabelle 2. Physicochemical properties of the parent mesoporous aluminosilicates (PMesoAS) and ZSM-5-coated mesoporous aluminosilicates (ZCMesoAS) samples before and after hydrothermal treatments.

Entry	Materials	Treatment time [h]	S_{BET} [m^{2}g^{-1}]	S_{BJH} [m^{2}g^{-1}]	Mesopore volume [cm^{3}g^{-1}]	BJH pore diameter [Å]
boiling water at 100°C						
1	PMesoAS-0-W[a]	0	1080	800	1.56	70
2	PMesoAS-48-W	48	415	375	1.72	120
3	ZCMesoAS-0-W	0	495	465	0.78	52
4	ZC MesoAS-48-W	48	475	485	0.85	55
5	ZC MesoAS-120-W	120	485	495	1.35	58
steaming of 20% vapor water in N_2 at 800°C						
6	ZCMesoAS-24-S	24	445	400	0.70	53

[a] PMesoAS-*x*-*y* where: *x* treatment time in hours, *y*: boiling water (W) or steaming (S) treatment.

  0044-8249/02/11406-1080 $ 17.50+.50/0

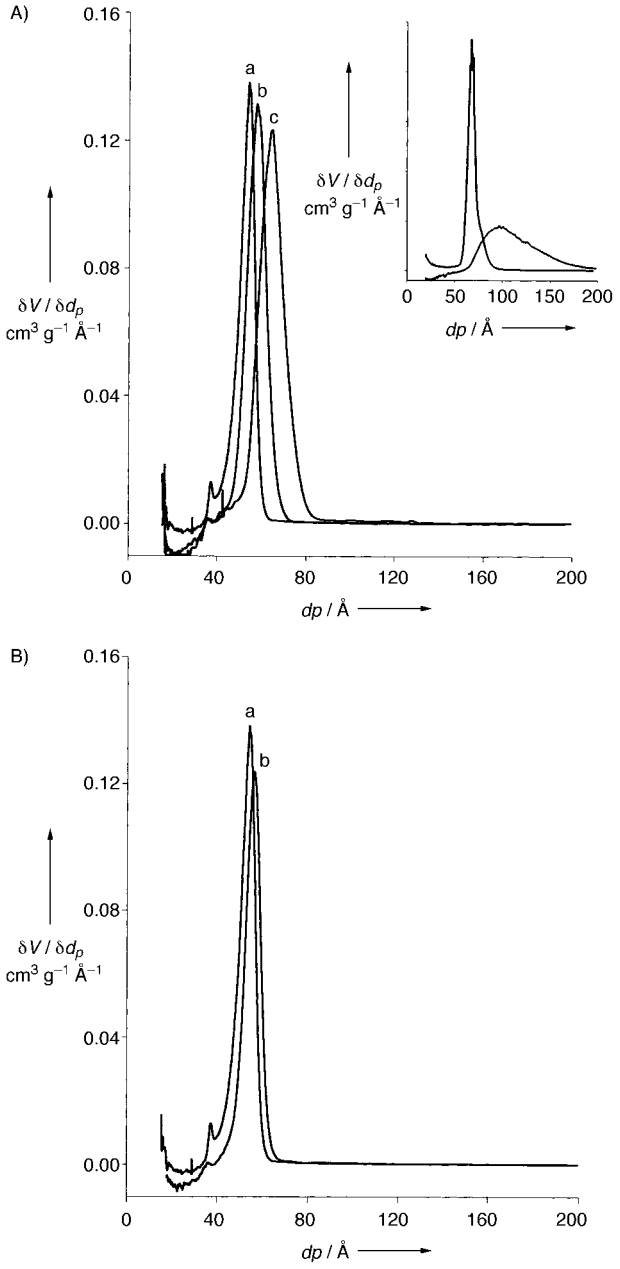

Figure 6. BJH pore diameter distributions calculated from the desorption branch of the isotherm for A) ZSM-5-coated MesoAS treated in boiling water at 100 °C: a) before and b) after treatment for 48 h and c) for 120 h (inset: the parent MesoAS sample treated in boiling water at 100 °C: a) before and b) after treatment for 48 h); and B) ZSM-5-coated MesoAS after steaming with 20% in N_2 at 800 °C: a) before and b) after steaming for 24 h.

still uniform. This indicates that the coated sample is much more hydrothermally stable than the conventional MesoAS sample. Furthermore, the coated sample was also steamed with 20% water vapor in N_2 at 800 °C for 24 h (Figure 6B). No essential change in the pore size distribution after steaming for 24 h indicates that the coated sample is hydrothermally ultrastable. We have performed a blank experiment in which the parent MesoAS was suspended in glycerol at 130 °C for 24 h. This treatment did not affect the specific surface area and pore diameter. This sample, however, did not show any improvement in hydrothermal stability compared to the parent MesoAS sample. The remarkable hydrothermal stability observed here involves therefore the zeolite seeds coated on the mesopore surface, which act to heal defect sites in the MesoAS framework. This is likely because the 2.8 nm sized ZSM-5 seeds templated by tetrapropylammonium (TPA) ions could electrostatically interact with tetrahedral Al sites in the silica framework and as consequence of this interaction, migrate inside the mesopore channels. It is indeed significant that any attempt at coating mesostructured silica with zeolite clusters in similar preparations failed. It is also apparent that this electrostatic interaction, which provides enough mobility to the zeolite nanoparticles for their initial migration within the mesopores, does not leave these nanoparticles with sufficient mobility for their sintering during crystallization. Calcination of these materials led to grafting nanoclustered ZSM-5 particles on the mesopore surface by the condensation reaction of silanol groups at the interface. Such a coating procedure reduces the concentration of silanols, as confirmed by the ^{29}Si MAS NMR results reported in Figure 5. Consequently, the high hydrothermal stability of the coated samples should be associated with this lowered silanol surface concentration since several treatments known to decrease the silanol concentration of MMS have been shown to improve their thermal and hydrothermal stability.[4] Finally, the strong acidity combined with an ultrastable, well-ordered uniform mesopore structure opens up new opportunities in the use of these coated materials as catalysts. These results also illustrate the potential importance of zeolite seeds as precursors for the design of this new class of materials. Indeed, our methodology is not limited to the coating by ZSM-5 seeds, since primary units with diameters of 2.8 nm for MFI/MEL structures, 2.6 nm for zeolite beta, 1.5 nm for ZSM-12, and 1.6 nm for zeolite sodalite have been reported.[13, 14] They can potentially be used to prepare a large variety of zeolite-coated mesoporous molecular sieves.

Experimental Section

Synthesis: The synthesis of zeolite-coated mesoporous materials involves two steps: the first step consists of the preparation of the mesoporous precursor and the desired clear zeolite gel; the second step is the coating of zeolite nanocrystals on the MMS surface using the diluted clear zeolite gel. In the first step: 1) An amorphous mesoporous alumosilicate precursor was synthesized from sodium silicate (28.7% SiO_2, 8.9% Na_2O) and sodium aluminate (46.78% Al_2O_3, 28.43% Na_2O) solutions as silicon and aluminum sources, respectively, using a poly(alkylene oxide) block copolymer $HO(CH_2CH_2O)_{20}(CH_2CH(CH_3)O)_{70}(CH_2CH(CH_3)O)_{20}H$ (Pluronic, P123 BASF) surfactant and sulfuric acid (98%). 2) Clear ZSM-5 gel solutions with desired chemical composition were synthesized from tetraethylorthosilicate (TEOS) and sodium aluminate as silicon and aluminum sources, respectively, and tetrapropylammonium hydroxide (TPAOH) as the zeolite template. In a typical ZSM-5 gel synthesis (atomic Si/Al = 10/1), a 20% aqueous solution of TPAOH (35 g) was added to TEOS (19.5 g). To the resulting clear solution, a solution of sodium aluminate (1.08 g; 46.78% Al_2O_3, 28.43% Na_2O) in distilled water (25 g) was added. The resulting clear solution was stirred for 24 h at room temperature to form protozeolitic species (known as zeolite seeds) and was finally diluted by distilled water to a volume of 600 mL.

In the second step, 20 g of the calcined mesoporous precursor was contacted with the diluted ZSM-5 gel (600 mL) prepared above under vigorous stirring at room temperature for 1 h. The solid sample was filtered, washed with distilled water, dried at 80 °C. The resulting solid was subsequently suspended in glycerol (50 mL) and the mixture was then

  0044-8249/02/11406-1081 $ 17.50+.50/0

transferred into a Teflon-lined autoclave and heated at 130 °C for 24 h. Glycerol was used as the medium for crystallization because due to the low solubility of silica in this medium, the framework was better retained during crystallization. Finally the solid product was filtered, washed with distilled water, dried at 80 °C, and calcined at 550 °C.

Characterization: Nitrogen adsorption/desorption isotherms at −196 °C were established by using an Omnisorp-100 apparatus. The specific surface area, S_{BET}, was determined from the linear part of the BET equation ($P/P_0 = 0.05 - 0.15$). The mesopore size distribution was calculated by using the desorption branch of the N_2 adsorption/desorption isotherms and the BJH formula. The mesopore surface area S_{BJH} and the mesopore volume V_{BJH} were obtained from the pore size distribution curves. The average mesopore diameter, D_{BJH}, was calculated as $4V_{BJH}/S_{BJH}$. Although its accuracy is limited, the BJH method, which is still universally utilized in the literature on mesoporous molecular sieves, yields results that may easily be compared with the current literature. High-resolution TEM images were obtained on a JEOL 200 CX transmission electron microscope operated at 120 kV. The samples for the TEM images were prepared by dispersing the fine powders of the products through a slurry in ethanol onto holey carbon copper grids. Solid-state ^{27}Al and ^{29}Si MAS NMR spectra were recorded at room temperature using a Bruker ASX 300 spectrometer.

Received: October 11, 2001 [Z18045]

[1] a) C. T. Kresge, M. E. Leonowicz, W. J. Roth, J. C. Vartuli, J. S. Beck, *Nature* **1992**, *359*, 710 – 712.

[2] a) D. Zhao, J. Feng, Q. Huo, N. Melosh, G. H. Fredrickson, B. F. Chmelka, G. D. Stucky, *Science* **1998**, *279*, 548 – 552; b) P. Yang, D. Zhao, D. I. Margolese, B. F. Chmelka, G. D. Stucky, *Nature* **1998**, *396*, 152.

[3] P. Schmidt-Winkel, W. W. Lukens, Jr., D. Zhao, P. Yang, B. F. Chmelka, G. D. Stucky, *J. Am. Chem. Soc.* **1999**, *121*, 254 – 255; P. Schmidt-Winkel, W. W. Lukens, J. P. Yang, D. I. Margolese, J. S. Lettow, J. Y. Ying, G. D. Stucky, *Chem. Mater.* **2000**, *12*, 686.

[4] D. Trong On, D. Giscard, C. Danumah, S. Kaliaguine, *Appl. Catal. A* **2001**, *222*, 299 – 357.

[5] A. Corma, *Chem. Rev.* **1997**, *97*, 2373.

[6] a) D. Trong On, P. N. Joshi, S. Kaliaguine, *J. Phys. Chem.* **1996**, *100*, 6743; b) E. Dumitriu, D. Trong On, S. Kaliaguine, *J. Catal.* **1997**, *170*, 150.

[7] a) D. Trong On, S. M. J. Zaidi, S. Kaliaguine, *Microporous Mesoporous Mater.* **1998**, *22*, 211; b) D. Trong On, M. P. Kapoor, P. N. Joshi, L. Bonneviot, S. Kaliaguine, *Catal. Lett.* **1997**, *44*, 171.

[8] A. Karlsson, M. Stocker, R. Schmidt, *Microporous Mesoporous Mater.* **1999**, *27*, 181.

[9] L. Huang, W. Guo, P. Deng, Z. Xue, Q. Li, *J. Phys. Chem. B* **2000**, *104*, 2817.

[10] a) Y. Liu, W. Zhang, T. J. Pinnavaia, *J. Am. Chem. Soc.* **2000**, *122*, 8791; b) Y. Liu, W. Zhang, T. J. Pinnavaia, *Angew. Chem.* **2001**, *113*, 1295; *Angew. Chem. Int. Ed.* **2001**, *40*, 1255.

[11] Z. Zhang, Y. Han, L. Zhu, R. Wang, Y. Yu, S. Qiu, D. Zhao, F.-S. Xiao, *Angew. Chem.* **2001**, *113*, 1298; *Angew. Chem. Int. Ed.* **2001**, *40*, 1258.

[12] a) D. Trong On, S. Kaliaguine, *Angew. Chem.* **2001**, *113*, 3348; *Angew. Chem. Int. Ed.* **2001**, *40*, 3248; b) D. Trong On, D. Lutic, S. Kaliaguine, *Microporous Mesoporous Mater.* **2001**, *44*, 435.

[13] a) C. E. A. Kirschhock, V. Buschmann, S. Kremer, R. Ravishankar, C. J. Y. Houssin, B. L. Mojet, R. A. van Santen, P. J. Grobet, P. A. Jacobs, J. A. Martens, *Angew. Chem.* **2001**, *113*, 2707; *Angew. Chem. Int. Ed.* **2001**, *40*, 2637; b) P. P. E. A. de Moor, T. P. M. Beelen, R. A. van Santen, L. W. Beck, M. E. Davis, *J. Phys. Chem. B* **2000**, *104*, 7600.

[14] P. P. E. A. de Moor, T. P. M. Beelen, B. U. Komanschek, L. W. Beck, P. Wagner, M. E. Davis, R. A. van Santen, *Chem. Eur. J.* **1999**, *5*, 2083.

[15] Z. Luan, C.-F. Cheng, W. Zhou, J. Klinowski, *J. Phys. Chem.* **1995**, *99*, 1019.

Diffusion-Limited, Aggregation-Based, Mesoscopic Assembly of Roughened Core – Shell Bimetallic Nanoparticles into Fractal Networks at the Air – Water Interface**

Yongdong Jin and Shaojun Dong*

The collective electronic, optical, and magnetic properties of organized assemblies of size-monodisperse nanocrystals are increasingly the subjects of investigation.[1] Control over the spatial arrangement of these building blocks often leads to new materials with chemical, mechanical, optical, or electronic properties distinctly different from those of their component parts.[2] Recently, metallic fractal clusters have sparked much interest because the localization of dynamical excitations in these fractal objects is a universal property which plays important roles in many physical processes.[3] In particular, the localization of resonant dipolar eigenmodes can lead to a dramatic enhancement of many optical effects in fractals.[3] For example, strongly fluctuating local fields in metallic fractal clusters can significantly exceed the external field and brings about a large enhancement of Raman scattering from the fractals.[4] Highly localized, laser-excited optical modes of silver colloid fractal clusters have been observed by photon scanning tunneling microscopy, and the results verify the main concepts of the resonant optical theory developed for fractal objects.[3] The localization of optical excitations and selective photomodification were also studied experimentally in fractal aggregates of silver colloidal nanoparticles.[5] These results prelude promising interesting applications, especially towards future nano-optics.[5, 6] Therefore, the synthesis of metallic fractal clusters is worthwhile for more detailed theoretical and technological studies.

In contrast to the wealth of recent theoretical work, experimental studies that can test the validity and applicability of modern theories have been rather sparse. In those studies performed, metallic fractal clusters were prepared from spherical colloidal particles by the addition of an adsorbate as a promoter (such as phthalazine,[3, 7] pyridine,[8] or gelatin,[5]) to the solution. Strictly speaking, these aggregates are three-dimensional in solution. However, they collapse upon drying to form nearly flat, two-dimensional (2D) structures. Indeed, it is quite likely that deposition and evaporation of the colloid onto the grid lead to additional aggregation. Herein, we report on a genuine aggregation-based strategy to prepare mesoscopic, two-dimensional fractal aggregates (even thin films) of bare (without adsorbate) silver/gold roughened core – shell nanoparticles by diffusion-limited aggregation (DLA) at the air – water interface by

[*] Prof. S. Dong, Dr. Y. Jin
State Key Laboratory of Electroanalytical Chemistry
Changchun Institute of Applied Chemistry
Chinese Academy of Sciences
Changchun 130022, Jilin (P.R. China)
Fax: (+86) 0431-5689711
E-mail: dongsj@ns.ciac.jl.cn.

[**] We gratefully acknowledge the National Natural Science Foundation of China (Grant Nos. 29835120, 29875028, 20075028) for support of this research and thank Prof. E. K. Wang for helpful discussions and generous support.

  0044-8249/02/11406-1082 $ 17.50+.50/0